International Journal of Pharmaceutics 420 (2011) 206–215

Contents lists available at SciVerse ScienceDirect

International Journal of Pharmaceutics

journal homepage: www.elsevier.com/locate/ijpharm

Short multi-armed polylysine-graft-polyamidoamine copolymer as efficient gene vectors

Shirong Pan[a,*], Chi Wang[a,b], Xin Zeng[a,b], Yuting Wen[a,b], Hongmei Wu[a,b], Min Feng[b,**]

[a] The First Affiliated Hospital, Sun Yetsen University, 58 2nd Zhongshan Road, Guangzhou 510080, PR China
[b] School of Pharmaceutical Sciences, Sun Yatsen University, 74 2nd Zhongshan Road, Guangzhou 510080, PR China

ARTICLE INFO

Article history:
Received 17 June 2011
Received in revised form 3 August 2011
Accepted 19 August 2011
Available online 27 August 2011

Keywords:
PAMAM-g-PLL
Gene vector
Gene transfection
Cytotoxicity
Complex

ABSTRACT

Polyamidoamine-polylysine graft copolymers (PAMAM-g-PLL) were prepared by ring-opening polymerization of benzyloxycarbonyl lysine *N*-carboxyanhydride (Lys(Z)-NCA) initiated with primary amine of generation 4 polyamidoamine (PAMAM G4) and subsequent deprotection of polyamidoamine-poly-(benzyloxycarbonyl lysine) copolymer (PAMAM-PLL(Z)). The chemical structure and composition of the PAMAM-g-PLL with varying length of PLL arms were characterized by Fourier transform infrared spectroscopy (FT-IR) and nuclear magnetic resonance spectroscopy (^{1}H NMR). Agarose gel electrophoresis test revealed that the PAMAM-g-PLL could completely combine DNA to form complexes. The scanning electronic microscopy (SEM) and atomic force microscopy (AFM) observation showed that the morphology of these complexes was spherical. Dynamic light scattering (DLS) measurement illustrated that the sizes of complexes were in range of 100–200 nm. The MTT assay demonstrated that cytotoxicity of PAMAM-g-PLL were lower than the either PAMAM G4 or the poly-L-lysine-15k (PLL-15k). The in vitro transfection test indicated that the PAMAM-g-PLL with 3.8 average polymerization degrees of PLL arms (PAMAM-PLL-3.8) displayed significantly higher transfection efficiency than that of PAMAM G4 and PLL-15k at the same N/P ratio, Furthermore, PAMAM-PLL-3.8 at the N/P of 40 or 80 displayed better serum-resistant capability than that of PEI-25k and Lipofectamine 2000. The DNA local delivery test in rabbit vessel exhibited that the restenosis was inhibited to a significant extent. The above facts revealed that PAMAM-PLL-3.8 is a promising gene vector with low cytotoxicity, high transfection efficiency and serum-resistant ability.

1. Introduction

Recently gene therapy attracted increasing interest, both viral and non-viral gene delivery systems were used in clinic trials to treat some human diseases. Among non-viral gene vectors, cationic polymers including PLL, chitosan, PEI, PAMAM dendrimer and their modified copolymers were widely applied to medical research (Braun et al., 2005; Sun and Zhang, 2010). But non-viral gene vectors had major problems such as certain cytotoxicity and relative low transfection efficiency that limited their in vivo application (Godbey et al., 1999; Duncan and Izzo, 2005). PAMAM dendrimer is a class of highly branched, narrowly dispersed macromolecules with well-defined structure and composition. The terminal primary amines of PAMAM dendrimer can easily be protonated, the positive charges on periphery can interact electrostatically with negative charges of phosphate groups in DNA, and condense the DNA molecules to form nanoscale compact complexes. The polycation/DNA complexes can protect the DNA from serum disruption during systemic circulation or nuclease degradation in endosome, and maintain the DNA molecule integrity in attaching the cell nucleus for gene expression. The inner tertiary amino groups with low pK_a can provide endosome good buffering capacity and benefit consequent transfection (Xue et al., 2006; Tian et al., 2006).

In order to apply PAMAM dendrimer for gene delivery system in vivo, further functionalization of PAMAM dendrimer is necessary. The primary amino groups, hydroxyl groups or carboxyl groups on the periphery of PAMAM can act as highly accessible sites for conjugating other functional groups, which provide probability for chemical modification. As constituents of proteins, amino acids are biocompatible, so amino acid-functionalization is an important approach for modification of PAMAM dendrimers. Amino acids containing more than 2 amino groups (including 2 amino groups) such as arginine, histidine, ornithine and lysine are preferentially used for the functionalization of PAMAM dendrimer, which can increase positively charge density and improve charge distribution on periphery of dendrimer, so that enhance the gene transfection efficiency and lower the cytotoxicity (Choi et al., 2004; Okuda et al., 2004). For example, di-arginine-conjugated PAMAM (G3 or

* Corresponding author. Tel.: +86 20 87330757; fax: +86 20 87330396.
** Corresponding author. Tel.: +86 20 39943119.
E-mail addresses: gzpshr@163.com (S. Pan), fengmin@mail.sysu.edu.cn (M. Feng).

0378-5173/$ – see front matter © 2011 Elsevier B.V. All rights reserved.
doi:10.1016/j.ijpharm.2011.08.036

G4) dendrimer through amide bonds could improve complex stability, intra-nuclear localization and transfection efficiency (Kim et al., 2009). Arginine-conjugated PAMAM-OH (G4) through ester bonds showed better transfection efficiency than PEI-25k and lower cytotoxicity than arginine-modified PAMAM G4 (Nam et al., 2009). Histidine-conjugated PAMAM G4 dendrimer through amide bonds could enhance transfection efficiency in 10% serum and reduce cytotoxicity in Bel 7402 or Hela cells (Wen et al., 2010). Ornithine-conjugated PAMAM G4 through amide bonds that contained 60 immobilized ornithine molecules could enhance the transfection efficiency in 10% fetal bovine serum (Kumar et al., 2010). In addition, conjugation of PAMAM-G4 with 19, 29 or 46 phenylalanine molecules resulted in ameliorative transfection efficiency (Navath et al., 2010).

PLL was used for gene carrier for a long time, but PLL/DNA delivery systems had lots of limitation in clinical application due to their relatively low transfection efficiency and moderate cytotoxicity. Recently PAMAM-PLL head–tail-type block copolymers (G2.5-PLL, G3.5-PLL and G4.5-PLL) were synthesized and the transfection efficiency of G3.5-PLL was also improved (Harada et al., 2009).

In the present study, PAMAM-g-PLL copolymers were prepared, and the copolymers were characterized by IR and ^{1}H NMR. The cytotoxicity of the PAMAM-g-PLL was evaluated by MTT assay, the particle size and morphology of complexes were inspected by DLS, SEM and AFM, respectively, the gene combining capability of copolymers was assessed through agarose gel electrophoresis, while the in vitro transfection efficiency was measured by flow cytometry. Finally the PAMAM-PLL-3.8/pVEGF165 complex was used for local delivery in rabbit vessel and the effect of preventing restenosis was evaluated.

2. Materials and methods

2.1. Materials

N-benzyloxycarbonyl-L-lysine (H-Lys(Z)-OH), 3-[4,5-dimethylthiazol-2-yl]-2,5-diphe-nyl-tetrazolium bromide (MTT), Lipofectamine 2000 were purchased from Sigma–Aldrich Inc. (St. Louis, MO USA). Methyl acrylate (MA), ethylene diamine (EDA), methanol, dimethyl formamide (DMF), tetrahydrofuran (THF), petroleum ether (bp 60–90 °C), chloroform were purchased from Guangzhou Reagent Inc. (Guangzhou China), which were distilled to remove any traces of water before use. Triphosgene was purchased from Shengtai Inc. (Zhejiang China). Fetal bovine serum (FBS) and RPMI 1640 culture medium were purchased from Invitrogen Gibco (USA). Dialysis tubing (MWCO 10,000 and 14,000) was purchased from Greenbird Inc. (Shanghai China).

2.2. Cell lines

Bel 7402, Hela and NIH 3T3 cell line were obtained from the animal center of Sun Yetsen University. Hek 293A cell line was purchased from the Invitrogen Life Technologies.

2.3. Plasmid DNA

Enhanced green fluorescent protein (EGFP) gene was a gift from West China University of Medical Sciences (Chengdu, China). Plasmid pEGFP-C1 containing the early promoter of CMV was amplified in competent *Escherichia coli* strain DH5α and purified by a Qiagen kit (Chatsworth, USA). pUC19-VEGF165 gene was a gift from Guangdong Provincial People's Hospital (Guangdong, China). VEGF165 gene segment with Hind III and BamH I sites was obtained from pUC19-VEGF165 by PCR which was cloned into pEGFP-C1. The recombinant plasmid pEGFP-VEGF165 was identified by sequence analysis, and the sequence of the recombinant plasmid DNA was consistent with hVEGF165 gene (AF486837) from Gene Bank.

2.4. Synthesis of PAMAM-g-PLL copolymers

2.4.1. PAMAM dendrimers

PAMAM was synthesized according to the procedures previously reported (Wu et al., 2011). Briefly excess MA/methanol solution was added to EDA/methanol solution and the mixture was stirred at 25 °C for 2 days (the Michael addition reaction). The solvent and excess MA were removed in vacuum to give a light yellow liquid that was denoted as PAMAM G(-0.5). Then the excess EDA/methanol solution was added to the PAMAM G-0.5/methanol solution and the mixture was stirred at 25 °C for 2 days (the amidation reaction). The solvent and excess EDA were removed in vacuum to give a yellow liquid that was denoted as PAMAM G0. Thus, the Michael addition reaction and the amidation reaction were alternatively repeated until the generation of PAMAM raised to 4. The water solution of crude product was dialyzed with dialysis tubing (MWCO 10,000) against distilled water for 16 h, finally lyophilized to give a yellow viscous liquid that was denoted as PAMAM G4.

2.4.2. Lys(Z)-NCA

Lys(Z)-NCA was prepared referring to the method reported in the literature (Harada and Kataoka, 2003). Briefly, H-Lys(Z)-OH was suspended in dried THF (1 g/10 mL), and triphosgene (1:1.2 by mol) was added. The suspension was stirred at 60 °C, 15 min later the solution turned to clear, after 30 min the reaction finished, and the product was precipitated with 10-fold volume of cold petroleum ether. Then the mixture was kept at −18 °C for 48 h, filtered, washed with petroleum ether and dried in vacuum. Finally a white crystalline, Lys(Z)-NCA was obtained.

2.4.3. PAMAM-g-PLL(Z)

As a macromolecule initiator DMF solution of PAMAM G4 was added to DMF solution of Lys(Z)-NCA (1 g/20 mL) at the NCA/NH_2 ratio of 3/1, 6/1 or 10/1 (by mol), respectively. The polymerization of Lys(Z)-NCA was performed based on a mechanism of the ring-opening polymerization. The reactant was stirring at room temperature for 72 h. The product was precipitated with 10-fold volume of distilled water, filtered and vacuum-dried. A white solid, PAMAM-g-PLL(Z) was obtained.

2.4.4. PAMAM-g-PLL

PAMAM-g-PLL(Z) was deprotected according to the method reported in the literature (Sun et al., 2007). Typically PAMAM-g-PLL(Z) was dissolved in anhydrous chloroform (5 g/100 mL), firstly a dry HCl gas was bubbling into the PAMAM-g-PLL(Z) solution for 40 min, then another dry HBr gas was bubbling into the solution for another 80 min, finally the reactant was standing overnight to ensure the complete deprotection (see Scheme 1). The mixture was precipitated with diethyl ether and filtered to give a yellow solid. The aqueous solution of the crude product was dialyzed with dialysis tubing (MWCO 14,000) against distilled water for 16 h and freeze-dried. Thus the PAMAM-g-PLL was obtained. PLL-15k was synthesized in the same procedures except using triethylamine as initiator.

2.5. Characterization of PAMAM-g-PLL copolymers

FT-IR spectra of PAMAM, PAMAM-g-PLL(Z) and PAMAM-g-PLL were measured on an EQUINOX55 Fourier transformation infrared spectrometer (Bruker, Germany). ^{1}H NMR spectra of PAMAM, PAMAM-g-PLL(Z) and PAMAM-g-PLL were determined using an AVANCE (400 MHz) NMR spectrometer (Bruker, Germany). MALDI-TOF mass spectrum of PAMAM-G4 were determined by

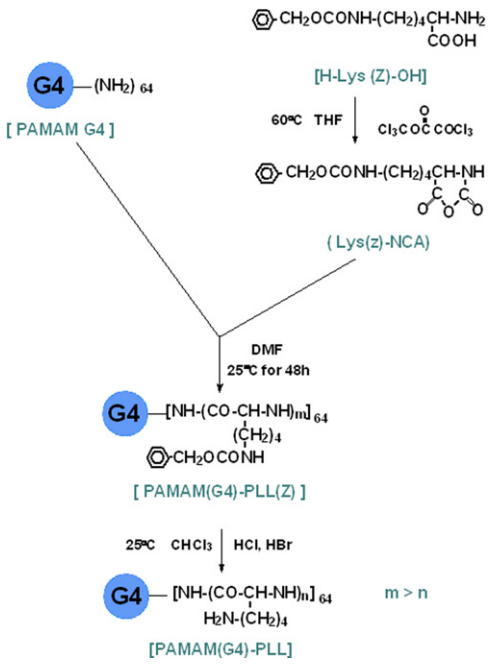

Scheme 1. The preparation processes of PAMAM-PLL copolymers.

a UltraflexIII-MALDI-TOF Mass Spectrometry (Bruker, Germany) using 2,5-dihydrobenzoic acid (DHB) as the matrix according to the literature (Muller et al., 2007). The number of the terminated primary amine groups of PAMAM G4 was determined by a potentiometric titrimeter using 0.1 mol/L HCl standard solution as the titration reagent according to the literature (Majoros et al., 2006).

2.6. Complexation of PAMAM-g-PLL with DNA

The complexes of PAMAM-g-PLL with DNA were self-assembled by adding appropriate volume of PAMAM-g-PLL solution to equal volume of 40 μg/mL of DNA solution, gently vortexing for a few seconds and incubating for 30 min at room temperature. The complexes were prepared in 150 mM NaCl at pH 7.4 for SEM observation, in 10 mM NaCl at pH 7.4 for DSL measurements or in PBS at pH 7.4 for other experiments. The concentration of the PAMAM-g-PLL solution was based on the chosen N/P ratios (here, N means the mol number of primary amines in PAMAM-g-PLL, P means the mol number of phosphates in DNA).

2.7. Agarose gel electrophoresis assays

The PAMAM-PLL/pEGFP-C1 complexes at the N/P ratios ranging from 0.05 to 10 were freshly prepared. 10 μL of the complexes were loaded into wells containing 1.0% agarose gel in TAE buffer with 0.5 μg/mL of ethidium bromides. Gel electrophoresis was subsequently performed at room temperature at 100 V for 60 min. DNA bands were visualized on an UV illuminator and photographed using a GAS7001X gel image system (UVITEC, USA).

2.8. Measurement of particle size and zeta potential

The PAMAM-PLL/pEGFP-C1 complex solutions at the N/P ratios ranging from 10 to 80 were freshly prepared. After incubating for 30 min, particle sizes and the zeta potential of the complexes were measured at room temperature by dynamic laser scattering (DLS) using a Nano ZS-90 Zetasizer (Malvern, UK). Meantime the particle size and morphology of the polymer/DNA complexes were also inspected using a JSM-6330F scanning electron microscope (SEM, Jeol Japan) and SPM-300HV atomic force microscope (AFM, Seiko Instrument Inc. Japan), respectively.

2.9. MTT assay

The cytotoxicity of PAMAM and PAMAM-g-PLL copolymers was evaluated based on the literature (Shcharbin et al., 2010). Bel 7402, Hela and NIH 3T3 cells were seeded in a 96-well plate at 2×10^4 cells/well in 200 μL of RPMI 1640 medium containing 10% FBS, respectively, and after incubating for 20–24 h the cells achieved 70–80% confluence. The growth media were replaced by 200 μL of polymer solutions with various concentrations, and cells were incubating for 6 h. All solutions were changed to fresh RPMI 1640 media, and cells were incubating for another 48 h. 15 μL of MTT solution (5 mg/mL in PBS) were added to each well, after 4 h of incubation the supernatants were aspirated, and 150 μL of DMSO were added to dissolve the formazan crystal formed by live cells. Finally the absorbance was measured at 570 nm by an ELISA microplate reader (Bio-Rad, USA). The cytotoxicity was expressed as relatively cell viability that was calculated according to the follows equation: cell viability (%) = $A_{test}/A_{control} \times 100\%$, here A_{test} and $A_{control}$ were absorbances for polymer or PBS, respectively.

2.10. In vitro transfection test

Bel-7402, Hela, NIH 3T3 and Hek 293 cells were seeded in a 24-well plate at 10^5 cells/well in 800 μL of RPMI 1640 media containing 10% FBS, respectively. After 20–28 h of growth the cells achieved 70–85% confluence. Prior to starting the transfection the PAMAM-PLL/pEGFP-C1 complexes with various N/P ratios were freshly prepared. At the beginning of transfection the media in wells were exchanged by 500 μL of fresh serum-free RPMI 1640 media, 200 μL of PAMAM-PLL/pEGFP-C1 complexes containing 2 μg of pEGFP-C1 were added into each well, and the cells were further incubating for 6 h. The solutions in wells were replaced with fresh media containing FBS, and the cells were incubating for another 48 h. After being observed and photographed on a fluorescence microscope, the cells were harvested from each well by the trypsin–EDTA treatment, and suspended in 200 μL of PBS (pH7.4). The percentages of EGFP expressing cells were measured to quantify the transfection efficiency using a BD-FACSAria System (Becton-Dickinson, USA). Transfection was carried out in triplicate. The procedures of transfection in 10% FBS were the same as described above, except at the beginning of transfection the media were exchanged by 500 μL of RPMI 1640 containing 10% FBS.

2.11. The local DNA delivery test in rabbit injured vessel

The test was performed according to previously published method (McArthur et al., 2001; Ando et al., 2004) and approved by the ethical committee of The First Affiliated Hospital, Sun Yetsen University. Prior to the test PAMAM-PLL-3.8/pPUC19-VEGF165 at N/P = 40 complexes was freshly prepared. 12 New Zealand white rabbits (2.5 ± 0.3 kg) were obtained from the animal center of Sun Yetsen University, and randomized into gene group and saline group (6 animals each group). The rabbits were anesthetized with 3% pentobarbital sodium (1 mL/kg weight) intravenously and ketamine hydrochloride (20 mg/kg weight) intramuscularly. A right incision on the neck was made to expose the right common carotid artery. The endothelium of right common carotid artery was denuded by three passages of an inflated 2F Fogarty catheter (Gore-Tex, Arizona USA).

A clip clamped the proximal site of the injured vessel temporarily to stop the blood flow, 200 μL of the DNA complex solution were injected into the injured vessel, and another clip clamped the distal site to allow the gene solution staying in the injured vessel

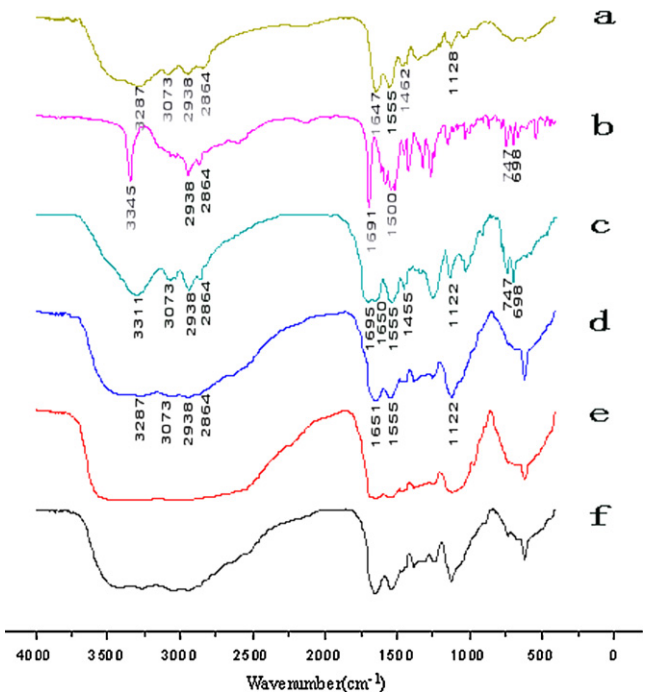

Fig. 1. FT-IR spectra of PAMAM-PLL copolymers: (a) PAMAM-G4, (b) H-Lys(Z)-OH, (c) PAMAM-PLL(Z), (d) PAMAM-PLL-2.1, (e) PAMAM-PLL-3.8, and (f) PAMAM-PLL-6.0.

for 30 mm. After perfusion finished, the clips were removed, the blood flow recovered, and the neck incision was closed. At 28 d of postoperation the animals were sacrificed and the segments of the perfused vessels were harvested. The specimens were ultra-thin-sectioned, stained with hematoxylin–eosin (HE) and inspected histologically. The areas of lumen (L), neointima (I) and media (M) on the sections were measured by BX51 Micro-Image Analysis System (Olympus, Japan), the I/M and $L/(L+I)$ values were calculated. The procedures of the saline group were the same as the gene group except 200 μL of saline were perfused in the injured vessel.

2.12. Statistical analysis

The experimental data were represented as means ± standard deviation, the variable P value between the groups means were evaluated using the student's t-test, when $P < 0.05$ the difference has considered statistical significance.

3. Results and discussion

3.1. Preparation and characterization of PAMAM-g-PLL copolymers

FT-IR spectrum of PAMAM G4 displayed a broad peak at 3287 cm^{-1} attributed to N–H stretching vibration of the terminal primary amine, a weak peak at 1462 cm^{-1} assigned to C–H shear bending vibration, and a weak peak at 1128 cm^{-1} corresponded to C–N stretching vibration of dendrimer framework (Fig. 1a). ^{1}H NMR spectrum of PAMAM G4 showed the peaks at 3.3, 2.9, 2.7 and 2.4 ppm belonged to CH_2 of different positions in the PAMAM dendrimer frame, respectively (Fig. 2a). The results of potentiometric titration showed that the number of the terminal primary amine of PAMAM G4 was 64.4, which is similar to the theoretical volume, 64.0. Based on MALDI-TOF mass spectra the M_w value of synthesized PAMAM G4 (13,051 Da) was consistent with the M_w value of PAMAM G4 purchased from Sigma–Aldrich (13,000 Da). The above results confirmed the formation of PAMAM G4.

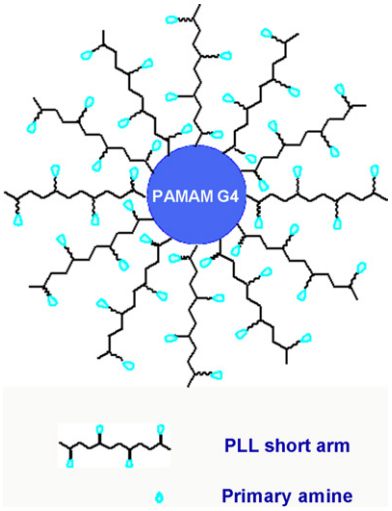

Scheme 2. The structure of the short multi-armed PLL graft PAMAM G4.

Polymerization of Lys(Z)-NCA was initiated by primary amine of PAMAM G4, thus PAMAM-g-PLL(Z) copolymers were synthesized. After deprotection the benzyloxylcarbonyl groups were converted to primary amino groups on PLL arms (Scheme 1). Actually, the PAMAM-g-PLL is a multi-armed-graft copolymer with the PAMAM G4 as a core and the PLL as short arms around the core (Scheme 2). In deprotection procedure, the PLL(Z) arm length further reduced mainly due to partial degradation in the acidic condition.

FT-IR spectra of PAMAM-g-PLL copolymers were seen in Fig. 1. For all samples the peak at 1650 cm^{-1} was belonged to C=O of amide (amide I) and peak at 1550 cm^{-1} was belonged to N–H of amide (amide II) (Huang et al., 2007). In Fig. 1b the peaks at 3345 and 2983 cm^{-1} were assigned to N–H symmetric and anti-symmetric stretching vibration at alpha carbon atoms, respectively (Bhadra et al., 2003). The peaks at 1691 and 1500 cm^{-1} were corresponded to C=C stretching vibration, but the double peaks at 747 and 698 cm^{-1} were corresponded to plane bending vibration of benzene ring (Refat et al., 2007), which were characteristic of the benzyloxylcarbonyl group. In Fig. 1c the peak at 3311 cm^{-1} was combination of the peak at 3287 cm^{-1} of Fig. 1a and the peak at 3345 cm^{-1} of Fig. 1b, a new peak at 3073 cm^{-1} appeared, and the peaks at 1691, 1500, 747 and 698 cm^{-1} still existed, which implied the formation of the PAMAM-g-PLL(Z). Fig. 1d, e and f were rather similar to each other, but the peaks at 2938–3287 cm^{-1} all became very broad, no peaks at 1691, 1500, 747 or 698 cm^{-1} were found, which indicated that complete deprotection of PAMAM-g-PLL(Z) occurred and a lot of primary amines generated.

^{1}H NMR spectra of PAMAM-g-PLL copolymers were shown in Fig. 2. In Fig. 2b the **k** peaks at 1.28–1.57 ppm were attributed to CH_2–CH_2–CH_2–CH_2 of H-Lys(Z)-OH (Tian et al., 2005), the **l** peak at 7.28 ppm was belonged to H atoms on benzene ring and **m** peak at 5.05 ppm was assigned to CH_2 of benzyloxylcarbonyl group. In Fig. 2c in addition to the **l**, **k** and **m** peaks, new **q** peak at 4.10 ppm corresponding to –NH–CH–CO– of polypeptide bonds (Huang et al., 2007; Bhadra et al., 2003) and new **p** peak at 3.5–2.0 ppm corresponding to all CH_2 of PAMAM framework appeared, which implied the formation of the PAMAM-g-PLL(Z). Fig. 2d, e and f were very similar to each other, the **l** and **m** peaks disappeared and the **k** peaks became stronger, which showed the benzyloxylcarbonyl groups were removed completely. The **a**–**i** peaks at 2.5–3.6 ppm were belonged to CH_2 of PAMAM framework, after deprotection the relative content of PAMAM increased, so the **a**–**i** peaks at 2.5–3.6 ppm became more obvious in comparison with Fig. 2c. The results confirmed the formation of PAMAM-g-PLL copolymers. The average

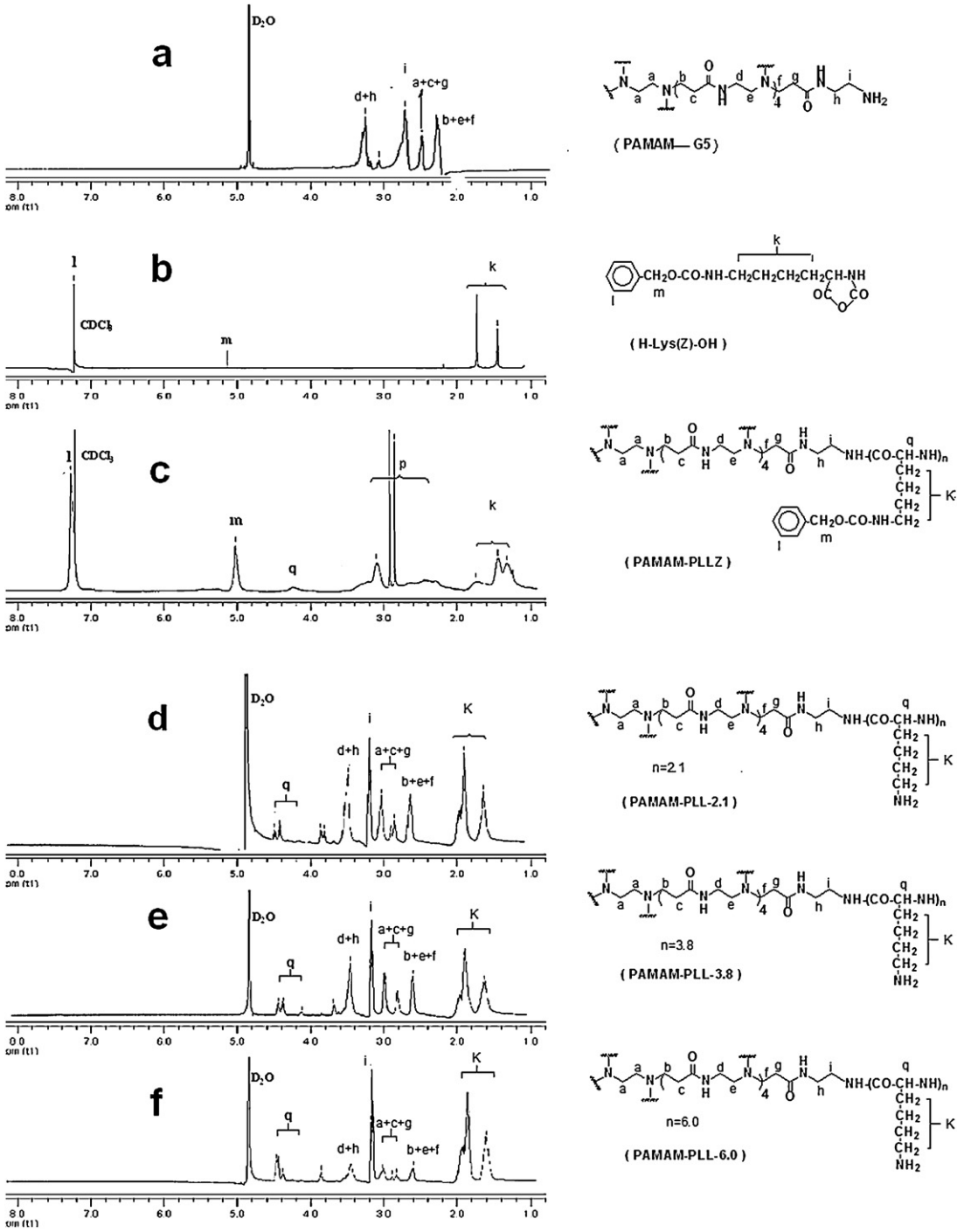

Fig. 2. ^{1}H NMR spectra of PAMAM-PLL copolymer: (a) PAMAM-G4, (b) H-Lys(Z)-OH, (c) PAMAM-PLL(Z), (d) PAMAM-PLL-2.1, (e) PAMAM-PLL-3.8, and (f) PAMAM-PLL-6.0.

Table 1
The composition and molecular weight of PAMAM-g-PLL copolymers.

Sample no.	Feeding ratio of NCA/NH_2 by mol	Yield of PAMAM-PLL	Average polymerization degree of PLL arms[a]	Total –NH_2 groups number of arms on periphery	M_n of PAMAM-PLL copolymers (kDa)
PAMAM-PLL-2.1	3/1	69%	2.1	135	30.3
PAMAM-PLL-3.8	6/1	60%	3.8	245	44.3
PAMAM-PLL-6.0	10/1	54%	6.0	384	62.5

[a] Determined by ^{1}H NMR.

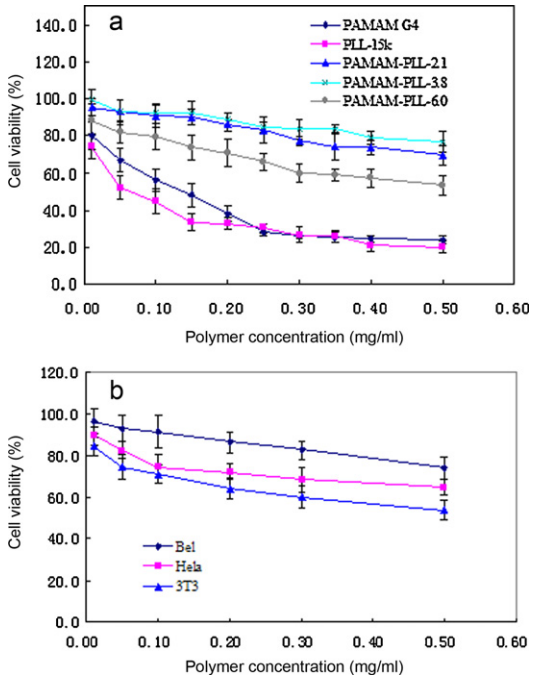

Fig. 3. Cytotoxicity assay: (a) cell viability of different polycations in the concentration range of 0.01–0.50 mg/mL and in Bel 7402 cell, and (b) cell viability of PAMAM-PLL-3.8 in different cells.

polymerization degrees of PLL short arms were calculated from area ratio of **a**–**i** peaks to **k** peaks. The data were listed in Table 1. The PAMAM-g-PLL copolymers with 2.1, 3.8 and 6.0 average polymerization degrees of PLL arms were expressed as PAMAM-PLL-2.1, PAMAM-PLL-3.8 and PAMAM-PLL-6.0, respectively.

3.2. Cytotoxicity of PAMAM-g-PLL copolymers

Generally, the cytotoxicity increased with an increase in the polymer concentration. As shown in Fig. 3a PAMAM G4 and PLL-1.5k exhibited moderate cytotoxicity. After grafting PLL short arms, the PAMAM-g-PLL displayed lower cytotoxicity than the PAMAM G4 or the PLL-15k homopolymer, and the PAMAM-PLL-3.8 and PAMAM-PLL-2.1 showed the least cytotoxicity among the polymers. The reason was that lysine was one component of body proteins, lysine oligomer showed less cytotoxicity than PLL with long chain, therefore PAMAM G4 grafted with PLL short arms (2–6 residues) would exhibit more biocompatible than unmodified PAMAM G4. In Fig. 3b PAMAM-PLL-3.8 showed different cytotoxicities in Bel 7402, Hela or NIH 3T3 cells illustrating the sensitivity of cytotoxicity to different cell species.

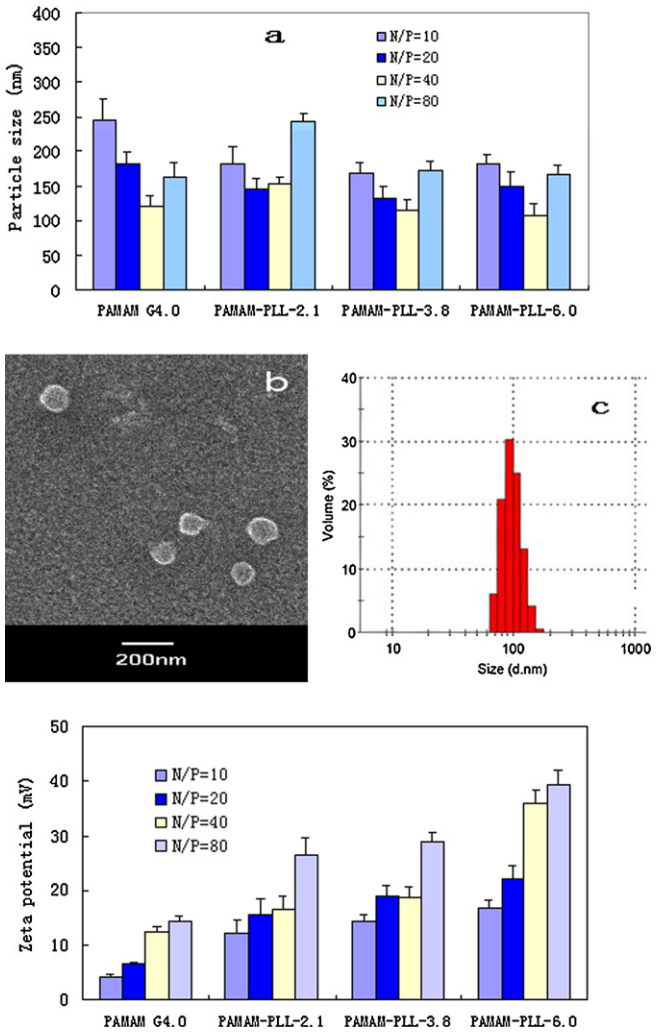

Fig. 5. (a) Particle size of polycation/DMA complexes at different N/P ratios, (b) SEM image of PAMAM-PLL-3.8/DNA complex at N/P = 40, (c) size distribution of PAMAM-PLL-3.8/DNA complex at N/P = 40 by DLS, and (d) zeta potential of polycation/DNA complexes.

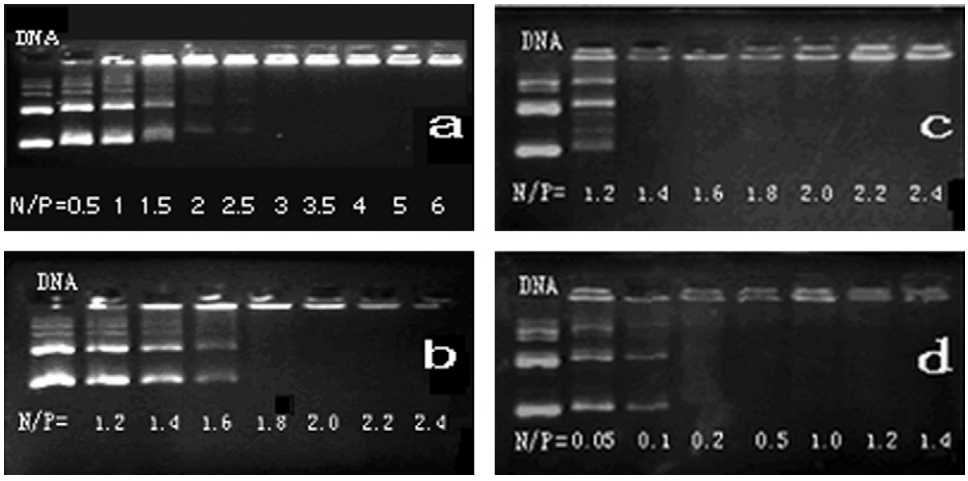

Fig. 4. Gel electrophoresis assay of polycation/gene complexes at various N/P ratios: (a) PAMAM-G4, (b) PAMAM-PLL-2.1, (c) PAMAM-PLL-3.8, and (d) PAMAM-PLL-6.0.

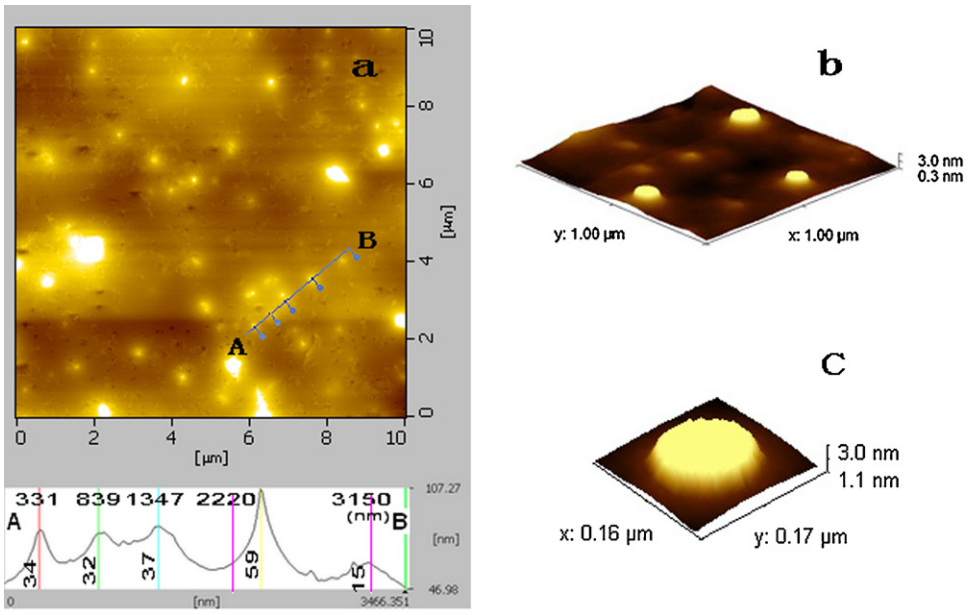

Fig. 6. AFM image of PAMAM-PLL-3.8/pDNA complex at N/P = 40: (a) (top) 2D view and (bottom) A–B section crossed five particles, (b) 3D view in range of 1000 nm, and (c) the 3D view in range of 160 nm.

3.3. DNA complexing capacity of PAMAM-g-PLL

Polycation can combine DNA through electrostatic effect, condense the DNA, and generate compact nanoscale particles or complexes. The good DNA complexing capacity is a necessary requirement for polycation gene carriers. Generally, the DNA complexing capacity of polycation was evaluated by agarose gel electrophoresis assay. In the method nude DNA molecules with various masses or conformations migrated to different distances in 100 V, so some DNA bands could be seen. But after complexing with polycation, the DNA negative charges were offset, and resulted in retardation of the DNA bands migration. As shown in Fig. 4 PAMAM G4, PAMAM-PLL-2.1, PAMAM-PLL-3.8 and PAMAM-PLL-6.0 began retard the DNA bands migration at the N/P ratio of 3.0, 1.8, 1.4 or 0.5, respectively. These results illustrated the order of the DNA complexing capacity was as follows: PAMAG4 < PAMAM-PLL-2.1 < PAMAM-PLL-3.8 < PAMAM-PLL-6.0. An explanation was that the structure like PAMAM grafted with PLL short arms could enhance the gene complexing capacity, and the longer the PLL arm, the larger the DNA complexing capacity. No visible precipitation was detected in the complexation of DNA with polycation.

3.4. Particle size and zeta potential of polycation/DNA complexes

The complexes sizes measured by DLS were shown in Fig. 5a. At the N/P of 10 the PAMAM-g-PLL copolymers could not condense DNA molecules completely, so larger and looser particles produced. As the N/P ratio increased the particle sizes decreased because more positive charges would enhance the DNA condensing capability and produce more compact particles. But at the N/P of 80 the particle size increased inversely because more positively charged PAMAM-PLL molecules were involved in the complexes at the N/P of 80 to generate the complexes with larger mass or sizes. The average particle sizes of PAMAM G4, PAMAM-PLL-2.1, PAMAM-PLL-3.8 and PAMAM-PLL-6.0 were 120 ± 16, 152 ± 16, 115 ± 15 or 106 ± 12 nm at the N/P of 40, respectively. It was seen from DLS that the size distribution of the complexes was unimodal (Fig. 5c). It was found from SEM that the morphology of the complexes looked like some round spheres (Fig. 5b).

Particle size and morphology of PAMAM-PLL-3.8/pDNA complexes were also studied by AFM. Fig. 6a (top) displayed the particle sizes in the range of 100–200 nm. Fig. 6a (bottom) exhibited an A–B section across five particles, in which the peak heights and distances between peaks were represented. Fig. 6b and c showed the 3D images of the particles. The AFM images confirmed the formation of complexes, and provided the more precise information about complex size and shape. The AFM results were also consistent with that of DLS and SEM.

The zeta potential of complexes is mainly depended on the N/P ratio or surface charges of complexes. As shown in Fig. 5d the zeta potential of complexes raised with increase of the N/P ratio. For different polycations an ascending order of zeta potential at the N/P of 40 was as follows: PAMAM G4 < PAMAM-PLL2.1 < PAMAM-PLL-3.8 < PAMAM-PLL-6.0 because the surface positive charges of complexes increased in the same order. The positive charges on complexes surface were of benefit to their attachment to cells and consequent endocytosis. The complexes of PAMAM-PLL-3.8 had appropriate particle size of 100–200 nm and positive zeta potentials of 10–20 mV, which were favorable for penetrating into cells and cellular uptake (Qi et al., 2009).

3.5. In vitro transfection efficiency of polycation/DNA complexes

Fig. 7a represented the transfection efficiency of PAMAM-PLL-3.8 and PAMAM G4 at optimum N/P ratio in different cells. The transfection efficiency related to the cell type, the descending order of the transfection efficiency was as follows: Hek 293 > Bel 7402 > Hela > NIH 3T3. It was worth noticing that the transfection efficiency of PAMAM-PLL-3.8 was always larger than that of PAMAM G4 in the same cell. Fig. 7b showed that as raising the N/P ratio from 20 to 40, the transfection efficiency was also increased because the higher positive charge density led to the stronger DNA complexing capability, at the N/P of 40 maximum transfection efficiency was achieved. However, at the N/P of 80 the transfection efficiency inversely reduced because very high positive charge density would cause serious cytotoxicity and a lot of cells death. In Fig. 8a the transfection efficiencies of PAMAM-PLL-3.8 at the N/P of 40 and 80 in serum-free medium in Hek 293 were $(52.1 \pm 0.2)\%$ or $(49.0 \pm 1.2)\%$, but the transfection efficiency of PAMAM G4,

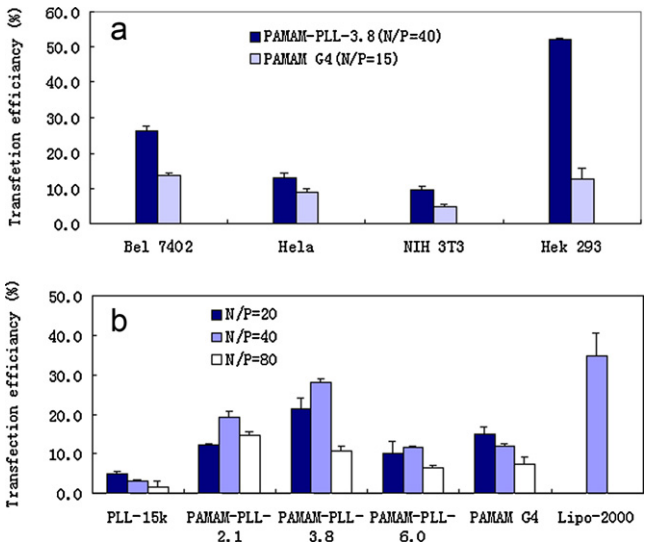

Fig. 7. (a) In vitro gene transfection efficiency of PAMAM-PLL-3.8/DNA complexes at N/P = 40 in different cells compared with PAMAM-G4/DNA complex at N/P = 15. (b) In vitro gene transfection efficiency of PAMAM-PLL/DNA complexes in Bel 7402 at different N/P ratios.

PEI-25k and Lipofectamine 2000 were (12.8 ± 2.9)%, (46.4 ± 4.3)% or (54.3 ± 7.8)%, respectively (at the optimal N/P ratio). The transfection efficiency of PAMAM-PLL-3.8 was much higher than that of PAMAM G4 ($^{*}P < 0.01$) and approached to that of PEI-25k or Lipofectamine 2000 ($^{***}P > 0.05$). For the same polycations the transfection efficiencies in serum-contained medium were always lower than that in serum-free medium because the serum could competitively combine with polycations and reduce the DNA complexing capacity. For PAMAM G4, PAMAM-PLL-3.8 at the N/P ratios of 40 and 80 the ratios of the transfection efficiencies with serum/without serum were 0.76/1, 0.65/1 or 0.81/1, however, for PEI-25k and Lipofectamine 2000 the ratios were only 0.09/1 or 0.06/1, respectively. The facts illustrated that PAMAM and PAMAM-g-PLL copolymers exhibited much higher serum-resistant capacity than PEI-25k or Lipofectamine ($^{**}P < 0.01$). In Fig. 8b the cells transfected in serum-free medium (row 2) showed more bright green fluorescent spots than that in 10% FBS-containing medium (row 4) especially for PEI-25k or Lipofectamine 2000. The fluorescence images were consistent with results of the flow cytometry (rows 1 and 3).

For linear PLL with high molecular weight the positive charges distribute along the long chain, which were not of benefit to complexing with DNA and improving the buffering capacity, therefore linear PLL long chains such as PLL-15k showed poor transfection

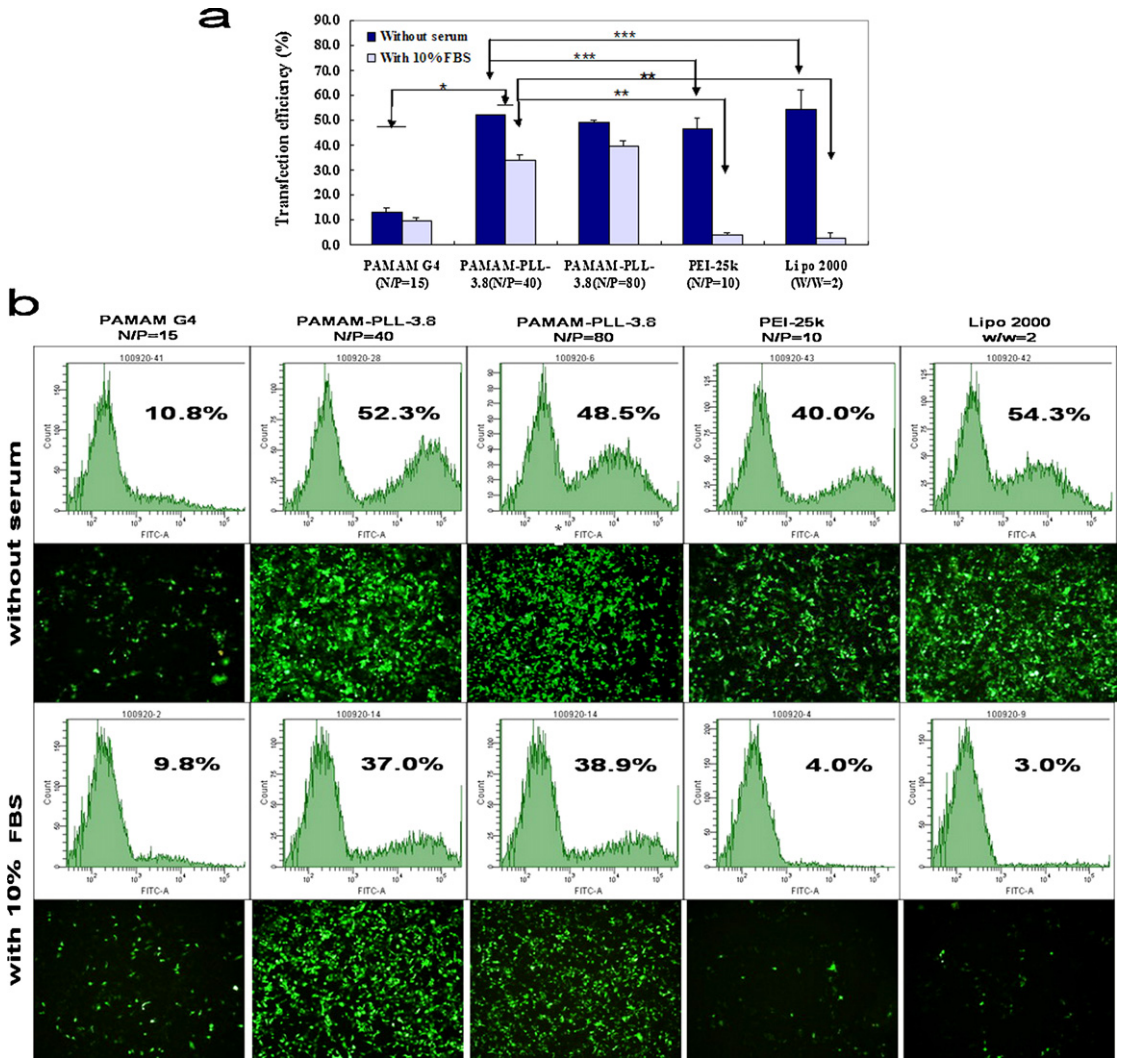

Fig. 8. (a) In vitro gene transfection efficiency of different polycation/pEGFP-Cl complexes in Hek 293 cells at optimal N/P ratio without serum for 6 h and with 10% FBS for 24 h, $^{*}P < 0.01$ and $^{**}P < 0.01$, the differences are considered statistical significance; $^{***}P > 0.05$, the differences are not considered statistical significance ($n = 3$). (b) Flow cytometry graphs and fluorescence images of different polycation/pEGFP-C1 complexes in Hek 293 cells, row 1 flow cytometry graphs without serum, row 2 fluorescence images without serum, row 3 flow cytometry graphs with 10% FBS, row 4 fluorescence images with 10% FBS.

Table 2
Histological section inspection of carotid artery after 28 d of gene local release in balloon-injury model.

Groups	Lumila area (L) (mm^2)	Intima area (I) (mm^2)	Media area (M) (mm^2)	I/M	$L/(L+I)$
Saline group	0.079 ± 0.059	0.267 ± 0.226	0.240 ± 0.179	1.11	0.23
Gene group	0.250 ± 0.147	0.092 ± 0.011	0.300 ± 0.061	0.31	0.73
	$^{*}P < 0.05$	$^{*}P < 0.01$	$^{*}P < 0.05$		

* Compared gene group with saline group ($n = 6$).

efficiency and moderate cytotoxicity. The PAMAM G4 had 64.4 terminal primary amines, so PAMAM-PLL-2.1, PAMAM-PLL-3.8 and PAMAM-PLL-6.0 had 135, 245 or 384 terminal primary amines which corresponded to that of PAMAM G5, G6 or G6-7, respectively (see Table 2). The more primary amines and the unique radial distribution of positive charge on the periphery could result in higher transfection efficiency. When the PAMAM-g-PLL copolymers complexed with DNA, the DNA molecules could locate between the PLL short arms and even extend into the internal cavities (Svenson and Tomalia, 2005) protecting the DNA from the attack of the serum molecules. It was the reason why PAMAM-PLL/DNA complexes displayed much better serum-resistant capacity than PEI-25k or Lipofectamine 2000.

3.6. Evaluation of preventing restenosis after local delivery of VEGF165 gene

Percutaneous transluminal coronary angioplasty (PTCA) is a minimal invasive technique for treatment of myocardial infarction. Despite high initial success rates, PTCA has still been limited to restenosis at the arterial injury site of 30–50% cases in 3–6 months of postoperation. Gene therapy is a new trial for preventing the restenosis. VEGF165 gene is an effective target gene (Deiner et al., 2006). Exogenous VEGF165 gene can be transfected and expressed in arterial cells to stimulate regeneration of the endothelial cells as well as to restrain over-proliferation of the smooth muscle cells, which would efficiently prevent restenosis.

In Fig. 9a we can see that the intima of the normal carotid artery was just a single layer of endothelial cells, and the media was mainly consisted of smooth muscle cells. When the intima was injured, over-proliferation of vessel cells would lead to neointima formation and media thickening. In the saline group a serious neointimal hyperplasia were found (Fig. 9b), but in the gene group a moderate neointimal hyperplasia occurred and the endothelium was almost recovered (Fig. 9c). The I/M value is a parameter to illustrate the extent of neointimal hyperplasia. The I/M value of gene group (0.31) was much less than that of saline group (1.11); the neointima area of the former was only 34% of the latter. The $L/(L+I)$ is another parameter to evaluate the patent extent of vessel. The $L/(L+I)$ value of the gene group (0.73) was also much larger than that of the saline group (0.23), and the lumen area of the former was 3.2 times larger than the latter (Table 2), which illustrated the stenosis extent of the gene group was lower than the saline group. We speculate that after the perfusion of complexes solution the complexes would enter into the vessel cells by internalization, and VEGF165 gene was transfected and expressed in nucleus, so that stimulating recovery of endothelium and inhibiting over-proliferation of smooth muscle cells.

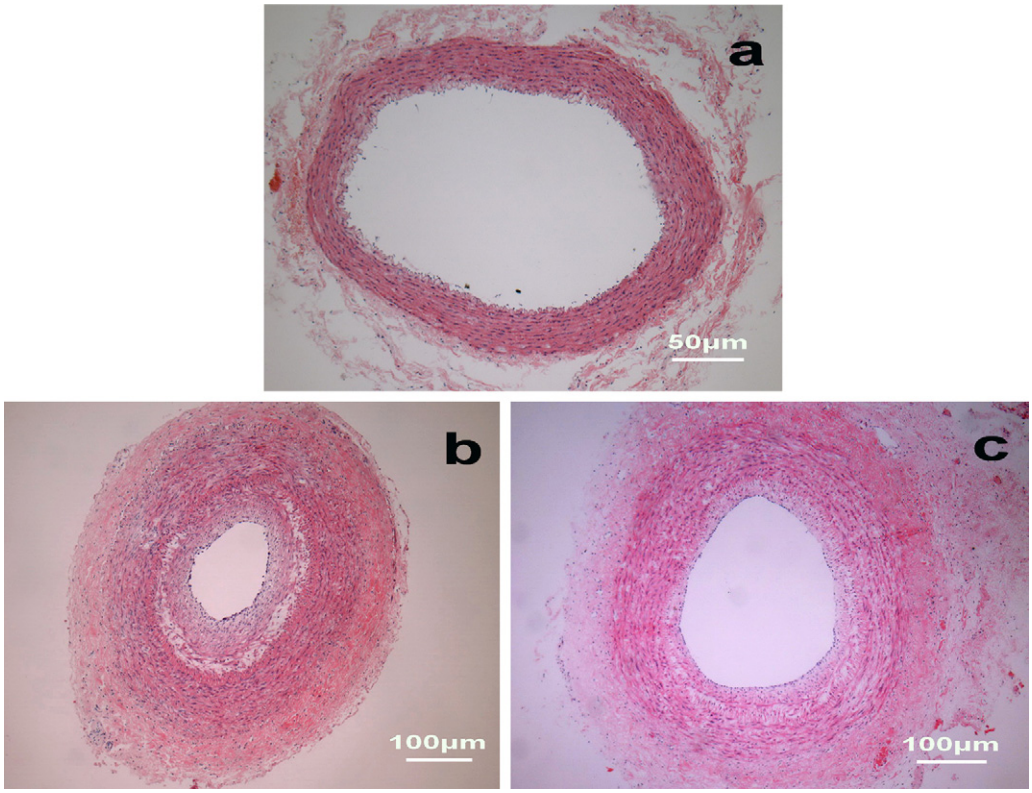

Fig. 9. Histological section of carotid artery after 28 d of gene perfusion in balloon-injury model (stained by HE): (a) normal artery (200×), (b) saline group (100×), and (c) gene group (100×).

4. Conclusion

PAMAM-g-PLL copolymers were prepared by polymerization of Lys(Z)-NCA using PAMAM G4 as macromolecular initiator and consequent deprotection of PAMAM-g-PLL(Z). The PAMAM-g-PLL copolymers exhibited less cytotoxicity. The PAMAM-g-PLL copolymers could complex with DNA to form nanocomplexes. The complex sizes were in the range of 100–200 nm and their zeta potentials were in the range of 10–20 mV. The higher positive charge density and unique radial charge distribution resulted in higher transfection efficiency than the PAMAM G4 or the PLL-15k and better serum-resistant capacity than PEI-25k or Lipofectamine 2000. The gene local delivery test in rabbit injured vessel showed that the restenosis was inhibited to a significant extent. PAMAM-g-PLL-3.8 will be a promising candidate as efficient gene vector.

Acknowledgments

The authors gratefully thank the National Natural Science Foundation of the People's Republic of China (30870618) for financial support in this study, and the Key Laboratory on Assisted Circulation, Ministry of Health for help in cell culture and gene transfection, etc.

Appendix A. Supplementary data

Supplementary data associated with this article can be found, in the online version, at doi:10.1016/j.ijpharm.2011.08.036.

References

Ando, H., Fukuda, N., Kotani, M., Yokoyama, S.-i., Kunimoto, S., Matrumoto, K., Saito, K., Kanmatsuse, S., Mugishima, H., 2004. Chimeric DNA–RNA hammerhead ribozyme targeting transforming growth factor-beta 1 mRNA inhibits neointima formation in rat carotid artery after balloon injury. Eur. J. Pharmacol. 483, 207–214.

Bhadra, D., Bhadra, S., Jain, S., Jain, N.K., 2003. A PEGylated dendritic nanoparticulate carrier of fluoro-uracil. Int. J. Pharm. 257, 111–124.

Braun, C.S., Vetro, J.A., Tomalia, D.A., Koe, G.S., Koe, J.G., Middaugh, C.R., 2005. Structure/function relationships of polyamidoamine/DNA dendrimers as gene delivery vehicles. J. Pharm. Sci. 94, 423–436.

Choi, J.S., Nam, K., Park, J.Y., Kim, J.B., Lee, J.K., Park, J.S., 2004. Enhanced transfection efficiency of PAMAM dendrimer by surface modification with L-arginine. J. Control. Release 99, 445–456.

Deiner, C., Schwimmbeck, P.L., Koehler, I.S., Loddenkemper, C., Noutsias, M., Nikol, S., Schultheiss, H.P., Ylä-Herttuala, S., Pels, K., 2006. Adventitial VEGF165 gene transfer prevents lumen loss through induction of positive arterial remodeling after PTCA in porcine coronary arteries. Atherosclerosis 189, 123–132.

Duncan, R., Izzo, L., 2005. Dendrimer biocompatibility and toxicity. Adv. Drug Deliver. Rev. 57, 2215–2237.

Godbey, W.T., Wu, K.K., Mikos, A.G., 1999. Poly(ethylenimine) and its role in gene delivery. J. Control. Release 60, 149–160.

Harada, A., Kataoka, K., 2003. Effect of charged segment length on physicochemical properties of core–shell type polyion complex micelles from block ionomers. Macromolecules 36, 4995–5001.

Harada, A., Kawamura, M., Kimura, Y., Takahashi, T., Kojima, C., Kono, K., 2009. Effect of head size in head–tail-type polycations on their in vitro performances as nonviral gene vectors. Macromol. Biosci. 9, 605–612.

Huang, H., Dong, C.M., Wei, Y., 2007. Biomimetic PAMAM-poly(benzyl L-glutamate) amphiphiles with multi-armed architecture: synthesis, physical properties and self-assembled nanoparticles. Comb. Chem. High Throughput Screening 10, 368–376.

Kim, T.-i., Cheng, Z.B., Nam, K., Park, J.S., 2009. Comparison between arginine conjugated PAMAM dendrimers with structural diversity for gene delivery systems. J. Control. Release 136, 132–139.

Kumar, A., Yellepeddi, V.K., Davies, G.E., Davies, G.E., Strychar, K.B., Palakurthi, S., 2010. Enhanced gene transfection efficiency by polyamidoamine (PAMAM) dendrimers modified with ornithine residues. Int. J. Pharm. 392, 294–303.

Majoros, I.J., Myc, A., Thomas, T., Mehta, C.B., Baker, J.R., 2006. PAMAM dendrimer-based multifunctional conjugate for cancer therapy: synthesis, characterization, and functionality. Biomacromolecules 7, 572–579.

McArthur, J.G., Qian, H.S., Citron, D., Banik, G.G., Lampher, L., Gyuris, G., Tsui, L., George, S.E., 2001. p27-p16 chimera: a superior antiproliferative for the prevention of neointimal hyperplasia. Mol. Ther. 3, 8–13.

Muller, R., Laschober, C., Szymanski, W.W., Allmaier, G., 2007. Determination of molecular weight, particle size, and density of high number generation PAMAM dendrimers using MALDI-TOF-MS and nES-GEMMA. Macromolecules 40, 5599–5605.

Nam, H.Y., Nam, K., Hahn, H.J., et al., 2009. Biodegradable PAMAM ester for enhanced transfection efficiency with low cytotoxicity. Biomaterials 30, 665–673.

Navath, R.S., Menjoge, A.R., Wang, B., Romero, R., Kannan, S., Kannan, R.M., 2010. Amino acid-functionalized dendrimers with heterobifunctional chemoselective peripheral groups for drug delivery applications. Biomacromolecules 11, 1544–1563.

Okuda, T., Sugiyama, A., Niidome, T., Aoyagi, H., 2004. Characters of dendritic poly(L-lysine) analogues with the terminal lysines replaced with arginines and histidines as gene carriers in vitro. Biomaterials 25, 537–544.

Qi, R., Gao, Y., Tang, Y., He, R.R., Liu, T.L., He, Y., Sun, S., Li, B.Y., Li, Y.B., Liu, G., 2009. PEG-conjugated PAMAM dendrimers mediate efficient intramuscular gene expression. Am. Assoc. Pharm. Sci. 11, 395–405.

Refat, M.S., El-Didamony, A.M., Grabchev, I., 2007. UV–vis, IR spectra and thermal studies of charge transfer complex formed between poly-(amidoamine) dendrimers and iodine. Spectrochim. Acta A: Mol. Biomol. Spectrosc. 67, 58–65.

Shcharbin, D., Pedziwiatr, E., Blasiak, J., Bryszewska, M., 2010. How to study dendriplexes II: transfection and cytotoxicity. J. Control. Release 141, 110–127.

Svenson, S., Tomalia, D.A., 2005. Dendrimers in biomedical applications–reflections on the field. Adv. Drug Deliver. Rev. 57, 2106–2129.

Sun, J., Chen, X., Deng, C., Yu, H.J., Xie, Z.G., Jing, X.B., 2007. Direct formation of giant vesicles from synthetic polypeptides. Langmuir 23, 8308–8315.

Sun, X.L., Zhang, N., 2010. Cationic polymer optimization for efficient gene delivery. Mini-Rev. Med. Chem. 10, 108–125.

Tian, H.Y., Deng, C., Lin, H., Sun, J.R., Deng, M.X., Chen, X.S., Jing, X.B., 2005. Biodegradable cationic PEG–PEI–PBLG hyperbranched block copolymer: synthesis and micelle characterization. Biomaterials 26, 4209–4217.

Tian, L., Nguyen, P., Hammond, P.T., 2006. Vesicular self-assembly of comb–dendritic block copolymers. Chem. Commun. (Camb.) 33, 3489–3491.

Wen, Y.T., Pan, S.R., Guo, Z.H., Wang, C., Zeng, X., Wu, H.M., Feng, M., 2010. Histidine modified PAMAM a s gene vector for enhancing gene transfection efficiency in serum. Chin. J. Biomed. Eng. 29, 129–136.

Wu, H.M., Pan, S.R., Chen, M.W., Wu, Y., Wang, C., Wen, Y.T., Zeng, X., Wu, C.B., 2011. A serum-resistant polyamidoamine-based polypeptide dendrimer for gene transfection. Biomaterials 32, 1619–1634.

Xue, Y.N., Liu, M., Peng, L., Huang, S.W., Zhuo, R.X., 2006. Improving gene delivery efficiency of bioreducible poly(amidoamine)s via grafting with dendritic poly(amidoamine)s. Macromol. Biosci. 10, 404–414.